

Study of Electron Bernstein Wave Emission on TST-2

SHIRAIWA Syun'ichi, NAGASHIMA Yoshihiko¹, USHIGOME Masayasu¹, KASUYA Naohiro¹, NOZATO Hideaki, KASAHARA Hiroshi, YAMADA Takuma¹, WADA Hirohumi, IJIMA Daisuke, KOBORI Yosuke, NISHI Tomoichiro, TANIGUCHI Tomokazu¹, EJIRI Akira and TAKASE Yuichi

Graduate School of Frontier Sciences, University of Tokyo

¹*Graduate School of Science, University of Tokyo*

(Received: 11 December 2001 / Accepted: 15 May 2002)

Abstract

Abstract: Electron Bernstein wave (EBW) emission, a possible alternative to the standard electron cyclotron emission diagnostic for overdense ($\omega_{pe} \gg \omega_{ce}$) plasmas, was studied on the TST-2 spherical tokamak. Simultaneous measurements of the radiation temperature and the density gradient at the upper hybrid resonance layer were carried out using a newly developed instrument consisting of a heterodyne radiometer combined with an AM reflectometer. It was found that the emission was fully unpolarized and the radiation temperature from the core region was about 150 to 200 eV. The mode-conversion efficiency was approximately 40 % which led to the estimated electron temperature of 250 to 370 eV.

Keywords:

EBW, spherical tokamak, temperature diagnostic

1. Introduction

Standard techniques for temperature diagnostic or heating and current drive based on the electron cyclotron wave (ECW) are not effective in ST, because ST plasmas are overdense and cannot sustain ECW. A promising option is to use the electron Bernstein wave (EBW), which has no density cutoff. For EBW is a short wavelength electrostatic wave, its optical thickness at the cyclotron resonance is high and can be considered to be black body emission.

A complexity associated with the use of EBW is that electrostatic wave cannot leave the plasma and must be mode-converted to an electromagnetic wave. The EBW undergoes mode-conversion near the upper hybrid resonance (UHR) to the X-mode to which access is possible via two scenarios. In the first scenario, first investigated by Preinhaelter and Kopeck'y in the early 1970's [1], the X-mode is mode-converted again to the O-mode. This scenario requires the optimum k_{\parallel} such that the locations of the O-mode cutoff and the high field

side cutoff coincide (B-X-O). In the second scenario, proposed more recently by Efthimion [2], the X-mode tunnels through the evanescent region between the UHR and the low field side cutoff (B-X-FX). In ST plasmas, the triplet composed of the high density cutoff, the UHR and the low density cutoff is formed within a few centimeters width (see Fig. 1), which makes the mode-conversion efficiency high

The B-X-FX power mode-conversion efficiency is given by [3]

$$C = 4e^{-\pi\eta}(1 - e^{-\pi\eta})\cos^2(\varphi), \quad (1)$$

where $\cos^2(\varphi)$ represents the interference effect between the high density cutoff and the UHR,

$$\eta = \frac{L_n \Omega}{c} \sqrt{\frac{\Omega}{\Omega + \omega_H}}$$

is the Budden parameter when the magnetic field is constant, L_n is the density scale length, ω_H is the upper hy-

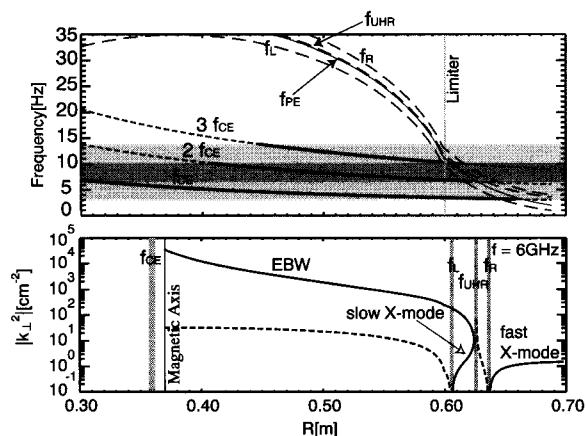


Fig. 1 Locations of critical layers and the perpendicular wave number for 6 GHz on TST-2. Parabolic profiles are assumed for the density and the temperature for the core plasma (inside the limiter radius) and an exponential decay for the scrape-off layer. The magnetic field on axis is 0.2 T, the central density is $1.0 \times 10^{19} \text{ m}^{-3}$ and the density at the limiter is $1.0 \times 10^{18} \text{ m}^{-3}$. The perpendicular wave-numbers drawn by dashed lines are evanescent waves.

brid frequency and Ω is the electron cyclotron frequency at the UHR. eq. (1) shows that the efficiency can be 100 % for optimum density scale length and phase factor. If a strong turbulence averages the phase factor, the average efficiency is simplified to $C_{\text{ave}} = 2e^{-\pi\eta}(1 - e^{-\pi\eta})$ and depends only on the density scale length.

So far, comparisons of the radiation temperature with the electron temperature carried out on CDX-U [4] and NSTX measured the density profile by Langmuir probes and Thomson scattering. However, Langmuir probes cannot be used in hot plasmas and Thomson scattering does not have a continuous temporal coverage. We have developed a new instrument that consists of a heterodyne radiometer and a reflectometer (radio-reflectometer) that can measure the radiation temperature and the density gradient simultaneously.

In the present paper, details of the newly built radio-reflectometer are described in Sec. 2. Section 3 is devoted to the description of initial results of the radio-reflectometer on TST-2. The results and perspectives are summarized in Sec. 4.

2. Radio-Reflectometer

In order to measure the density gradient of the region where the wave received by radiometer is mode-converted, the radiometer and reflectometer should share

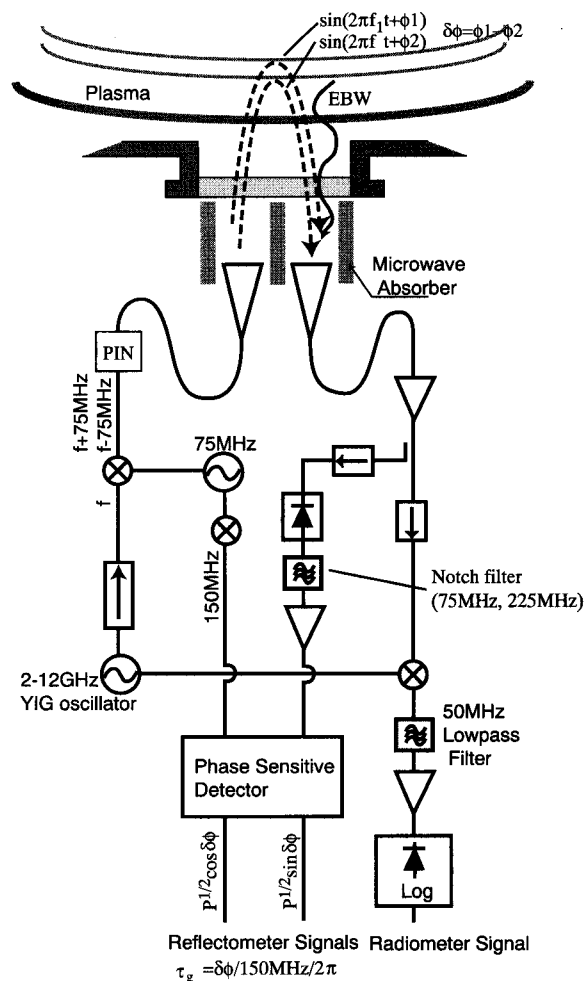


Fig. 2 Block diagram of the radio-reflectometer. The frequency coverage is from 5–12 GHz that corresponds the 2nd and 3rd harmonic emission from TST-2.

the receiving antenna. The difficulty of the sharing is that the probing wave of the reflectometer may be detected by radiometer. Using the different wave polarization for radiometer and reflectometer may offer a solution. However, the reflected wave from plasma was found to contain nearly 10 % cross-polarized component. A better way is to use two frequencies and to make the frequency difference greater than the radiometer bandwidth. Hence, we employ the amplitude modulated reflectometry [5].

A block diagram of the radio-reflectometer is shown in Fig. 2. It has a single microwave YIG oscillator that is fed to two mixers. The first one is used to generate probing waves of slightly different frequencies. Representing the YIG oscillator frequency

by F, the launched wave frequencies are $F+75$ MHz and $F-75$ MHz. The probing waves are amplified to power levels of about 15 dBm and fed to the ridged horn antenna whose frequency range is 5 to 18 GHz. The mixture of the reflected waves and the EBW emission are received by the second ridged horn antenna, amplified by 33 dB and fed to the second mixer and the diode detector.

The second mixer is used to detect the EBW emission. Since the bandwidth of mixer's IF port is 300 MHz, the output of the second mixer contains the emission in the frequency range from $F-300$ MHz to $F+300$ MHz and the intense reflected wave components at DC, 75 MHz and its harmonics. The bandpass filter composed by a 50 MHz low pass filter and a 3 MHz high pass filter at the input stage of the logarithmic amplifier is used to eliminate the reflected wave components and reduce the radiometer bandwidth to 100 MHz (Double Side Band detection). Finally, the logarithmic amplifier, Analog Devices AD8307, detects the filtered EBW signals. The radial resolution determined by the bandwidth is about 5 mm. The radiometer is calibrated using liquid nitrogen.

A diode detector is used to detect the beat signal between two probing waves at 150 MHz. Contribution produced by mixing other harmonics generated at the first mixer such as $F+150$ MHz and F are less than -30 dB in power and are negligible. A diode detector produces the frequency components such as 75 MHz and 225 MHz. A filter is used to eliminate them. With the local signal generated by the frequency doubler, the phase sensitive detector performs quadrature phase detection and the phase delay of the beat wave is obtained.

3. Experimental setup and results

The radio-reflectometer is installed at the low field side mid-plane of the TST-2 [6]. TST-2 is a small spherical tokamak with major radius $R=0.36$ m, minor radius $a = 0.23$ m, aspect ratio $A\sim 1.6$ and elongation $\kappa\sim 1.3\text{--}1.8$. We measured the ohmic plasmas with plasma current of 80 kA, discharge duration of 20 ms, ion temperature of 50–100 eV and toroidal field of 0.15 to 0.2 T. As shown in Fig. 1, the plasmas are calculated to be overdense except in the very peripheral region and mode-conversion takes place near the limiter surface.

We locate the antennas 90 cm away from the vacuum window for two reasons. The first reason is to suppress the interference effect of the reflectometer. The closer the antennas are located to the window, the

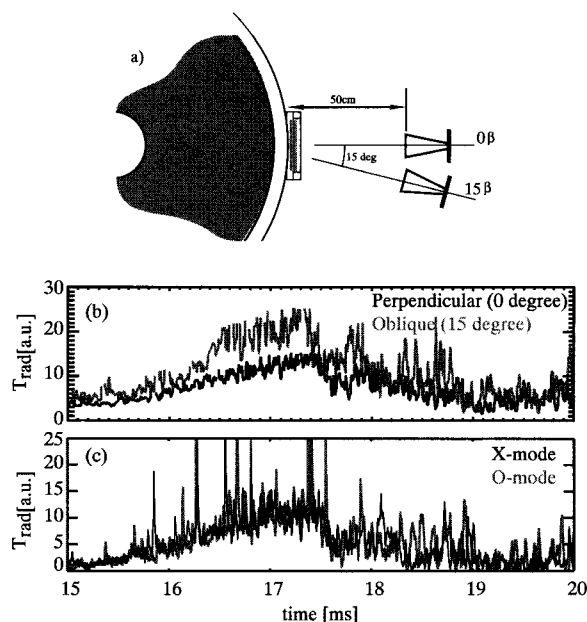


Fig. 3 Comparisons of EBW emission for different receiving antenna orientation and polarizations. (a) the antenna arrangement (b) X-mode emission in the direction perpendicular to flux surface (black) is smaller than emission in the oblique direction (gray). (c) X-mode (black) and O-mode (gray) have the same intensity.

greater the solid angle that the antennas view the plasma and the interference of waves reflected at various parts of the plasma surface becomes more serious. The second reason is to restrict the range of the parallel wave number received by the radiometer to as close to zero as possible. This is because higher X-mode emission were detected at an oblique angle ($k_{\parallel} \neq 0$) than in the normal direction ($k_{\parallel} = 0$) (Fig. 3(b)), when the antenna was located 50cm away from the window.

The plasma current, the measured 3rd harmonic EBW emission from the core region and the phase delay of the reflectometer of typical discharge are shown in Fig. 4. Several sudden drops of emission coincide with reconnection events, while the reflectometer signal shows no obvious change. It is inferred that the emission drop represents the core temperature decrease. By sweeping the YIG oscillator frequency by shot by shot manner, the spectrum of EBW emission and density profile around the UHR were measured. Figure 5 shows the spatial profile of EBW emission obtained by mapping the frequency to the radial location. It is shown that the 3rd harmonic emission from the core plasma is 100 to 150 eV and monotonically decreases as minor

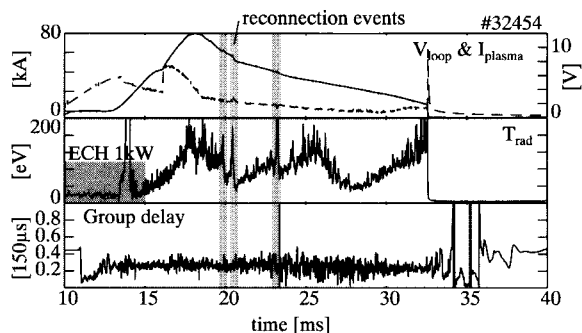


Fig. 4 Temporal evolution of radiometer signal and the phase of reflectometer. The frequency of the radio-reflectometer is 11 GHz.

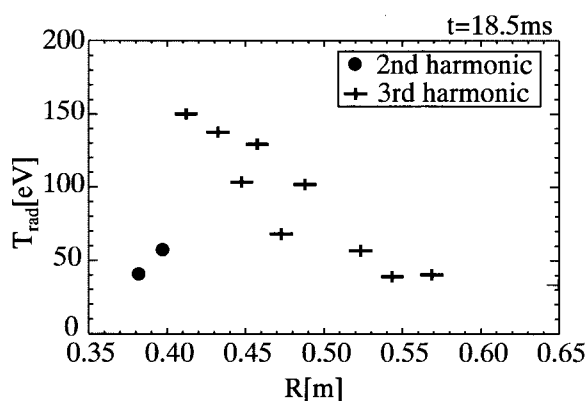


Fig. 5 Spatial profile of EBW emission at $t=18.5$ ms. In order to map the frequency to the radial location, the $1/R$ dependence of the toroidal field and a linear spatial profile of the poloidal field are assumed.

radius increases. Using WKB approximation for the sake of simplicity, the density scale length of about 3 cm is obtained. The mode-conversion efficiency calculated from eq. (1) is about 40 % and leads to the central electron temperature of 250 to 370 eV.

In the B-X-FX scenario, the evanescent region is narrowest for $k_{\parallel}=0$ and mode-conversion becomes most efficient. Hence, the result shown in Fig. 3(b) seems to contradict the one dimensional mode-conversion theory. Another contradictory result is shown in Fig. 3(c), in which O-mode emission has almost the same intensity as X-mode emission. The phenomena shown in Fig. 3(b) and (c) are not thoroughly understood. A possibility is that multiple reflection between the plasma and the

vacuum vessel have randomized the wave number spectrum and polarization.

Presently, a full wave treatment is under preparation for precise reconstruction of the density profile, because the wavelength of the probing wave is comparable to the measured density scale length. As an independent absolute electron temperature measurement, Thomson scattering is also under preparation.

4. Conclusion

In this paper, we report the newly constructed EBW emission diagnostic that consists of a radiometer and an AM reflectometer. The instrument is installed on TST-2 and the radiation temperatures of the 2nd and 3rd harmonic emission and the density scale length are, for the first time, measured simultaneously. Initial results show that the radiation temperature is about 100 to 150 eV in the plasma core. The density scale length of about 3 cm was obtained from reflectometer using the WKB approximation. The calculated mode-conversion efficiency is about 40 %, resulting in the estimated electron temperature of 250 to 370 eV.

Acknowledgments

The one of authors (S.S) is grateful to Dr. Gary Taylor, Dr. Phil Efthimion and Dr. Brent Jones for piles of discussions and advices which have significant importance for conducting the EBW research on TST-2.

References

- [1] J. Preinhaelter and V. Kopeck'y, *J. Plasma Phys.* **10**, 1, (1973)
- [2] P.C. Efthimion, J.C. Hosea, R. Kaita, R. Majeski and G. Taylor, *Rev. Sci. Instrum.* **70**, 1018 (1999).
- [3] A.K. Ram and S.D. Schultz, *Phys. Plasmas* **7**, 4084 (2000).
- [4] G. Taylor, P.C. Efthimion, B. Jones, T. Munsat, J.C. Hosea, R. Kaita, R. Majeski, R.W. Harvey and S. Shiraiwa, *Bull. Am. Phys. Soc.* **46**, 307, (2001).
- [5] J. Sánchez, B. Brañas, E. de la Luna, T. Estrada and V. Zhuravlev, *Rev. Sci. Instrum.* **63**, 4654 (1992).
- [6] Y. Takase, A. Ejiri, N. Kasuya, T. Mashiko, S. Shiraiwa, L.M. Tozawa, T. Akizuki, H. Kasahara, Y. Nagashima, H. Nozato, H. Wada, H. Yamada, T. Yamada and K. Yamagishi, *Nucl. Fusion* **41**, 1543 (2001).